의학박사 학위논문

새로운 *KCNQ4* 돌연 변이의 발견 및 난청 유형 분석

Characteristics of novel *KCNQ4* variants showing a distinct hearing loss phenotype

2017년 8월

서울대학교 대학원
의학과 중개의학 전공
박 미 나

의학박사 학위논문

새로운 *KCNQ4* 돌연 변이의 발견 및 난청 유형 분석

Characteristics of novel *KCNQ4* variants showing a distinct hearing loss phenotype

2017년 8월

서울대학교 대학원
의학과 중개의학 전공
박 미 나

새로운 *KCNQ4* 돌연 변이의 발견 및 난청 유형 분석

Characteristics of novel *KCNQ4* variants showing a distinct hearing loss phenotype

지도교수 오 승 하

이 논문을 의학과 박사학위논문으로 제출함

2017 년 4 월

서울대학교 대학원

의학과 중개의학 전공

박 미 나

박미나의 박사학위논문을 인준함

2017 년 7 월

위 원 장 이 준 호 (인)

부 위 원 장 오 승 하 (인)

위 원 구 자 원 (인)

위 원 김 성 준 (인)

위 원 강 동 묵 (인)

Characteristics of novel *KCNQ4* variants showing a distinct hearing loss phenotype

by Mina Park

A Thesis Submitted to the Department of Translational Biomedical Research in Partial Fulfillment of the Requirements for the Degree of Doctor of Philosophy in Medicine (Translational Biomedical Research) at the Seoul National University College of Medicine

April, 2017

Approved by thesis committee:

Chairman	Jun Ho Lee
Vice Chairman	Seung Ha Oh
Member	Ja-Won Koo
Member	Sung Joon Kim
Member	Tong Mook Kang

Abstract

Characteristics of novel KCNQ4 variants showing a distinct hearing loss phenotype

Mina Park

Department of Translational Biomedical Research

The graduate School

Seoul National University

KCNQ4 mutations lead to autosomal dominant non-syndromic, and typically progressive and high-frequency, hearing loss (HL). In this report, I identified two novel KCNQ4 mutations, namely p.R331Q and p.811_816del, in two different families. One mutation in the C-terminal region was associated with low- to mid-frequency HL and the other mutation, located in the P-loop, was associated with high frequency HL. Although I did not observe a difference in the subcellular localization of the KCNQ4 mutants p.R331Q and c.811_816del, c.811_816del protein expression was significantly decreased compared with that of wild-type KCNQ4 (KCNQ4WT) and the p.R331Q mutant. The potassium currents were significantly decreased in both the p.R331Q and c.811_816del mutants compared with KCNQ4WT, indicative of the pathogenic potential of the two variants. Based on

electrophysiological data, p.R331Q and c.811_816del KCNQ4 channels showed loss of function and a dominant-negative effect when combined with functional KCNQ4WT channels. The heteromeric mutant channels assembled with WT were activated by a KCNQ4 activator (retigabine), and the degree of rescue by retigabine was stronger in the p.R331Q heteromer than in the c.811_816del heteromer. This study reports a C-terminal tail variant among KCNQ4 mutants for the first time, and broadens the audiologic phenotypic spectrum from high frequency sensorineural HL to include low- to mid-frequency sensorineural HL.

Key words: Hearing loss, KCNQ4, K^+channel, Mutation, Dominant negative effect, Rescue

Student Number: 2014-30928

Contents

Abstract ---------- i

Contents ---------- iii

List of Figures ---------- iv

Introduction ---------- 1

Materials and Methods ---------- 2

Results ---------- 9

Discussion ---------- 16

References ---------- 20

Figures ---------- 24

Abstract (Korean) ---------- 33

Acknowledgement ---------- 34

List of Figures

Figure 1. Clinical information for each KCNQ4 mutant. ---------- 24

Figure 2. Sanger sequencing traces for two mutants. ---------- 25

Figure 3. Intracellular chemistry for wild-type *KCNQ4* (*KCNQ4*WT), the p.R331Q and c.811__816del mutations. ---------- 26

Figure 4. Qualitative and quantitative expression analysis for KCNQ4WT, p.R331Q and c.811__816del mutations. ---------- 27

Figure 5. Outward K+ currents recorded from HEK293 cells transiently expressed with human KCNQ4 channels. ---------- 28

Figure 6. Linopirdine-sensitive current measured in heteromeric p.R331Q KCNQ4 channels. ---------- 29

Figure 7. Linopirdine-sensitive current measured in heteromeric c.811__816del KCNQ4 channels. ---------- 30

Figure 8. Activation of heteromeric p.R331Q mutant channels by retigabine, a KCNQ channel activator. ---------- 31

Figure 9. Activation of heteromeric c.811__816del mutant channels by retigabine, a KCNQ channel activator. ---------- 32

Introduction

The KCNQ4 gene is associated with autosomal dominant non-syndromic hearing loss (HL) (DFNA2) [1-4], and 21 mutations of KCNQ4 have been identified [5, 6]. The majority of these mutations are located in the pore region and show an association with progressive high-frequency HL [5, 6]. KCNQ4 is expressed with longitudinal (from base to apex) as well as radial (from inner hair cells [IHCs] to outer hair cells [OHCS]) gradients in the cochlea [7]. KCNQ4 is dominant in OHCs at the apex of the cochlea, and in IHCs and spiral ganglions (SGs) at the base. KCNQ4 mutations cause progressive high-frequency HL due to the dysfunctional KCNQ4_v3 variant in SGs and IHCs at the base of the cochlea [7].

KCNQ4 protein functions as a voltage-gated potassium channel, consisting of six transmembrane domains (S1 - S6) and a pore (P)-loop located between S5 and S6 [6]. Functionally, it forms a channel pore consisting of the P-loop domain [6] and a long intracytoplasmic tail. The P-loop, a tetramer composed of six domains, allows the passage of potassium ions, and the long tail plays a regulatory role in channel gating and tetramer assembly.

In this report, I describe two novel KCNQ4 mutations; one of these mutations was associated with low- to mid-frequency HL, and the other with high frequency HL. Based on these results, I expanded the phenotypic spectrum based on novel KCNQ4 mutations.

Materials and Methods

Subjects

All procedures in our study were approved by the Institutional Review Board of Seoul National University Bundang Hospital (IRB B-1007-105-402). Written informed consent was obtained from each individual (or caregiver in the case of children). Two subjects (SB62-110 and SB155-271) showed moderate autosomal dominant sensorineural HL and were included in our study. Medical and developmental history, and physical examination and pure tone audiometry (PTA) results, were evaluated for phenotype validation.

Audiometric evaluation

PTA with air and bone conduction thresholds of 0.25, 0.5, 1, 2, 4, and 8 kHz was administered to three subjects according to standard protocols. Low-, mid-, and high-frequency tones were in the range of 250 - 500 Hz, 1 - 2 kHz, and 4 - 8 kHz, respectively. I calculated the mean hearing threshold for the low-, mid-, and high-frequency tones [8].

Molecular genetic diagnosis

Targeted exon sequencing of 129 reported deafness genes (TES-129) from two subjects (SB62-110 and SB155-271) was performed by Otogenetics (Norcross, GA, USA). The acquired reads were aligned

with the UCSC reference genome sequence (hg19) and variants were acquired. Further bioinformatic analyses were performed as described previously [9]. Briefly, data were filtered to identify candidate single-nucleotide polymorphisms (SNPs) that may be associated with non-syndromic sensorineural HL. During the first filtering step, non-synonymous SNPs with read depths > 40 were chosen. The SNPs were compared and traced based on the single nucleotide polymorphism (dbSNP build 138) and our databases. Novel SNPs, as well as SNPs associated with known diseases, were identified. Next, the genetic inheritance of the subjects was explored; SNPs that were not associated with the genetic inheritance of the affected individual were excluded. Then, I confirmed that the selected SNPs were present in the two families using Sanger sequencing and inspected an additional 426 unrelated Korean control chromosomes.

The pathogenicity of the missense mutation of subject SB62-110, and the deletion variant of the other subject (SB155-271), were investigated using SIFT and Polyphen-2. To measure the evolutionally preserved amino acid sequence, I applied GERP++ grade in the UCSC Genome web site (http://genome.ucsc.edu/).

Plasmid construction

Wild-type (WT) KCNQ4 cDNA was cloned into the SgfI and KgockI sites of pEGFP-N1.

Cell culture and transient transfection

The monkey embryonic kidney cell line COS-7 (Korean Culture Line Bank, Seoul, Korea) was maintained in Dulbecco ′ s modified Eagle ′ s medium (DMEM) with 10% fetal bovine serum. Before transient transfection, cells were planted to a density of 70 - 80% confluency in a Lab-Tek II chamber (Nunc, Rochester, NY, USA). Cells were transfected with Lipofectamine 3000 (Invitrogen, Seoul, Korea) and incubated at 37°C for 24 hours. Cells were then stained with concanavalin A [10].

Intracellular chemistry

After incubation, transfected cells were fixed in 4% paraformaldehyde for 15 min followed by washing with phosphate-buffered saline (PBS), which was repeated three times. Cells were incubated in primary antibodies (ANTI-FLAG; Sigma Aldrich Corp., St. Louis, MO, USA) at 24°C for 160 min, washed with chilled (4°C) PBS three times, and incubated in secondary antibodies [F(ab′)2-Goat anti-Mouse IgG (H+L), Invitrogen, Seoul, Korea] at room temperature for 90 min. Slides were mounted with VECTASHIELD mounting medium (Vector Laboratories, Burlingame, CA, USA) and images were taken using a confocal microscope (LSM710; Carl Zeiss, Jena, Germany).

Western blot

HEK293 cells were transiently transfected with various combinations of KCNQ4 plasmids (WT, p.R331Q, and p.811_816del) using

Lipofectamine Plus reagent (Life Technologies, Inc., Carlsbad, CA, USA) and harvested after 24 h post-transfection. To prepare the total protein fraction, cells were lysed with RiPA buffer (25 mM Tris • HCl pH 7.6, 150 mM NaCl, 1% NP-40, 1% sodium deoxycholate, and 0.1% SDS). Cytosolic and membrane fractions were separated from transfected cells using the Membrane Fractionation kit (Abcam, Cambridge, UK). The protein concentration of each fraction was determined using a bicinchoninic acid (BCA) assay (Thermo Scientific, Waltham, MA, USA). Protein (30 μg) was loaded onto a sodium dodecyl sulfate polyacrylamide gel electrophoresis (SDS-PAGE) gel, transferred to a nitrocellulose membrane (Millipore, Billerica, MA, USA), and subjected to Western blot analysis with anti-FLAG (1:10,000; Sigma), anti-β-actin (1:2,000; Santa Cruz Biotechnologies, Santa Cruz, CA, USA), and anti-Na^+ K^+ ATPase (1:20,000; Abcam) antibodies. Bound antibodies were detected using horseradish peroxidase (HRP)-conjugated secondary antibodies and the Chemiluminescent Substrate kit (Thermo Scientific). Images were captured using the ImageQuant LAS4000 mini system (GE Healthcare, Milwaukee, WI, USA).

Electrophysiology

External bath solution and internal pipette solution

The external bath solution for whole-cell voltage clamp recording consisted of (in mM): 145 NaCl, 5 KCl, 1.5 CaCl2, 1 MgCl2, 10

HEPES, and 10D-glucose; pH was adjusted to 7.4 with N-methyl-D-glucamine (NMDG). The internal patch pipette solution contained (in mM): 145 KCl, 10 NaCl, 5 EGTA, 3 Mg-ATP, and 10 HEPES; pH was adjusted to 7.2 with KOH.

Chemicals

All chemicals were purchased from Sigma unless otherwise stated. Linopirdine (1,3-Dihydro-1-phenyl-3,3-bis(4-pyridinylmethyl)-2H-indol-2-one) and retigabine (ezogabine, N-(2-Amino-4-(4-fluorobenzylamino)phenyl) carbamic acid ethyl ester) were dissolved in dimethyl sulfoxide (DMSO) and prepared as 20 mM and 30 mM stock solutions, respectively. Each stock solution was diluted in an external bath solution before use.

Whole-cell voltage clamp

Transiently transfected HEK293 cells were placed on a poly (L-Lysine)-coated recording chamber mounted on an inverted microscope (IX-70; Olympus, Tokyo, Japan) and the external bath solution was perfused continuously at a rate of 2 ml/min. A healthy-looking cell with (green fluorescent protein; GFP) was selected for whole-cell patch-clamp recording. All recordings were performed at room temperature (~23oC). Patch electrodes were removed from borosilicate glass tubing (WPI, Sarasota, FL, USA) and the pipette tip was fire-polished with a microforge (MF-83;

Narishige, Tokyo, Japan). The final pipette tip resistance was 1.5~3 MΩ when filled with the internal pipette solution. After achieving conventional whole-cell patch clamp configuration, whole cell K^+ currents were amplified and recorded with an Axopatch 1D amplifier (Axon Instruments, Foster City, CA, USA). All current recordings were acquired and analyzed using Clampex software (pCLAMP 7.0; Axon Instruments). The currents were filtered at 5 kHz and acquired at a sampling rate of 5 kHz. Before acquiring the ionic currents, series resistance was compensated for and the cell membrane capacitance was measured and cancelled using a circuit of the patch-clamp amplifier. With a holding potential of -80 mV, KCNQ4 currents were generated with a 2-sec depolarizing voltage step, which ranged from -70 to +60 mV in 10 mV increments, followed by a 1 sec hyperpolarizing voltage step to -50 mV. Step voltage pulses were generated at 10-sec intervals. After recording the whole-cell K^+ current, linopirdine (10 μM) or retigabine (30 μM) was administrated to the cells and linopirdine-sensitive or retigabine-sensitive components were obtained by digital subtraction. For comparison, whole-cell current densities (pA/pF) were calculated by dividing the KCNQ4 steady-state current amplitudes (obtained at +50 mV) by the measured cell membrane capacitance (pF).

Data analysis and statistics

In all recordings, amplitudes of the steady-state KCNQ4 currents measured 2 sec after each depolarizing voltage step were analyzed.

To evaluate the voltage dependence of KCNQ4 currents, the conductance-voltage relationship was fitted to a Boltzmann function with the following equation:

$$I = Imax / [1+ exp((V1/2-Vm)/S)]$$

where V1/2 is the half-activation voltage and S is the slope factor. Calculated values are expressed as means ± standard error of the mean (SEM). The data were plotted and analyzed with Origin software (ver. 6.1; Origin Lab Corp., Northampton, MA, USA). Statistical significance was determined for paired and unpaired Student's t- tests and a P value < 0.05 was considered significant.

Result

Clinical features of three KCNQ4 mutants

The pedigrees of SB62-110 and SB155-271 indicate a typical autosomal dominant heredity form of HL (Fig. 1A). Clinical histories and audiograms of two of the patients showed progressive, bilateral and symmetrical sensorineural HL. However, one of these patients showed low- to-mid frequency HL and the other showed high-frequency HL (Fig. 1B). Neither patient showed clinical symptoms of vestibular dysfunction.

Identification of novel mutations in the KCNQ4 gene

Sanger sequencing of the KCNQ4 gene revealed two novel mutants including missense (c.G992 > A) and deletion (c.811_816del) variants (Fig. 2 A and B). The novel missense variant (p.R331Q), located in the long cytoplasmic C-terminus, caused a guanine to adenine transition at nucleotide position 992 (c.G992 > A), resulting in the substitution of arginine for glutamine (unlike for other mutants reported previously [5]). This residue was highly conserved among KCNQ4 orthologs and paralogs (http://genome.ucsc.edu/) (Fig. 2C). Another variant (c.811_816del), located in the P-loop similar to other mutants reported previously [5], caused a deletion of six nucleic acids (GCCGAC) and resulted in loss of alanine and aspartic acid. The

GCCGAC residue was conserved in the patient's father and mother (Fig. 2B), showing that c.811_816del is a *de novo* mutant.

Mutant trafficking

To determine whether loss of function was due to an abnormal subcellular localization of mutant proteins, we performed intracellular trafficking of p.R331Q and c.811_816del. Based on qualitative and quantitative analysis, there was no difference in the subcellular localization of the two KCNQ4 mutants compared with that of WT (Fig. 3).

Protein expression

To explore the effect of p.R331Q and c.811_816del on membrane protein synthesis, I performed western blotting. In the total fraction, the expression of p.R331Q was comparable to that of WT; meanwhile, c.811_816del showed low protein expression. The KCNQ4 expression level in the cytosol fraction of WT, p.R331Q, and c.811_816del showed no difference, and that in the membrane fraction was similar to that in the total fraction. This indicated that protein in the total fraction originated from the membrane fraction (Fig. 4A, 4A´). Similar to WT, I observed increased p.R331Q and c.811_816del protein expression (Fig. 4B, 4B´). To distinguish between the heterozygous state in patients with predominantly inherited HL, WT and mutant KCNQ4 cDNA were co-transfected using WT and two KCNQ4 mutants. Regarding the cotransfection of WT and p.R331Q, there was no

difference in protein level according to the mix ratio. Regarding the cotransfection of WT and c.811_816del, the expression level decreased according to an increase in the proportion of c.811_816del (Fig. 4C, 4C´). To explore the degradation pathway of the WT and two KCNQ4 mutants, I added MG132 (protease inhibitor), which is degraded via the ubiquitin-proteasome pathway. There was no difference in expression according to the amount of MG132 in the WT, p.R331Q, and c.811_816del strains. This suggests that KCNQ4 protein is not metabolized through the ubiquitin-proteasome pathway (Fig. 4D, 4D´).

Effects of the two KCNQ4 mutants on channel function

Electrophysiological analysis of p.R331Q and c.811_816del mutants

For functional analysis, the WT KCNQ4 (KCNQ4WT) and two novel KCNQ4 mutants (KCNQ4p.R331Q and KCNQ4c.811_816del) were transiently expressed in HEK293 cells, and ionic currents generated by the channels were studied using whole-cell patch clamp recording. HEK293 cells transfected with empty pCMV6 vector and GFP were used as the control group (GFP) and the control currents were compared with KCNQ4-mediated currents.

KCNQ4WT-expressing HEK293 cells generated a slowly activating and outwardly rectifying K^+ current in response to the applied step pulses, ranging from -70 to +60 mV (Fig. 4A and 4B). In contrast,

cells transfected with either KCNQ4p.R331Q or KCNQ4c.811_816del showed a relatively small transient outward current under the same conditions, resembling the K^+ current observed in GFP-transfected HEK293 cells (Fig. 5A and 5B). Current densities obtained at +50 mV were 36.72 ± 5.22 in KCNQ4WT, 11.80 ± 1.15 in GFP, 14.49 ± 1.16 in p.R331Q, and 16.32 ± 1.66 in c.811_816del. KCNQ4WT current density was significantly higher than that of the other three groups (Fig. 5C, $p < 0.05$).

To isolate the KCNQ4 channel-mediated K^+ current from the total ionic current, which is given by the sum of the endogenous HEK293 cell K^+ current and the expressed KCNQ4 current, I used linopirdine, a common KCNQ2–5 channel blocker. After > 5 min of treatment with 10 μM linopirdine, linopirdine-sensitive K^+ currents were digitally subtracted from total K^+ currents (Figs. 6A and 7A). As shown in Figs. 6B and 7B, the current-voltage (I-V) curve of the linopirdine-sensitive components recorded in KCNQ4WT showed a clear outwardly rectifying current. The current density (pA/pF) of KCNQ4WT measured at +50 mV was significantly ($p < 0.05$) higher than that of the two mutants and GFP (WT = 81.92 ± 18.32, p.R331Q = 5.58 ± 1.25, c.811_816del = 5.30 ± 0.94, GFP = 3.45 ± 0.55 pA/pF) (Figs. 6C and 7C). These data suggest that the two novel KCNQ4 mutants found in our Korean patients are loss-of-function phenotypes.

Dominant-negative effects of p.R331Q and

c.811_816del

To replicate the heteromeric assembly observed in our patients, the cDNA of KCNQ4WT and the KCNQ4 mutants was co-expressed at various molar ratios (WT : mutant ratio range: 0:4 - 4:0) and the resultant K^+ currents were analyzed (Figs. 6 and 7). As described above, neither the p.R331Q nor c.811_816del mutant channel showed a linopirdine-sensitive K^+ current when expressed alone (WT : mutant ratio = 0:4).

When the p.R331Q mutant was co-expressed with WT at ratios of 3:1, 2:2, 1:3, and 0:4, the linopirdine-sensitive KCNQ4 currents (at +50 mV) were 18.55 ± 5.88, 13.58 ± 3.61, 8.80 ± 2.08, and 5.58 ± 1.25 pA/pF, respectively (Fig. 6C). The heteromeric KCNQ4 currents were significantly smaller than the homomeric WT current (81.92 ± 18.32, $p < 0.05$). In addition, heteromeric channels with WT : p.R331Q ratios of 2:2 and 1:3 showed a higher K^+ current versus GFP-expressing cells (Fig. 6C, $p < 0.05$). When the c.811_816del mutant was co-expressed with WT at ratios (of 3:1, 2:2, 1:3, and 0:4, the linopirdine-sensitive KCNQ4 currents (at +50 mV) were 40.74 ± 11.46, 14.81 ± 5.60, 11.51 ± 5.06, and 5.30 ± 0.94 pA/pF, respectively (Fig. 7C). Excluding the 3:1 group, the heteromeric combination (1:3 and 0:4) had a current that was significantly lower than the homomeric WT current (Fig. 7C, $p < 0.05$). In addition, the heteromeric current at the 3:1 ratio showed a higher amplitude than that of GFP (Fig. 7C, $p < 0.05$). Overall, for the heteromeric KCNQ4 currents, there

was an association between a lower amplitude and a greater amount of transfected mutant cDNA (Figs. 6 and 7). These data suggest that p.R331Q and c.811_816del mutants have dominant-negative effects when they are assembled with KCNQ4WT channels.

Activation of p.R331Q and c.811_816del mutant channels by retigabine

It is important to determine whether the two KCNQ4 mutant channels are activated by pharmacological drugs. To explore this, retigabine (30 μM), a common KCNQ2 - 5 family activator, was applied to HEK293 cells expressing homomeric or heteromeric KCNQ4 mutant channels. For comparison, KCNQ4WT and GFP-transfected cells were used as a positive and negative control, respectively (Figs. 8 and 9). After treating the cells with 30 μM retigabine for > 3 min, retigabine-sensitive K^+ currents were digitally subtracted and the voltage-dependence of the currents was evaluated using I-V curves (Figs. 8B and 9B).

As in previous reports (Figs. 6 and 7), the p.R331Q or c811_816del mutant was co-expressed with KCNQ4WT at various ratios, and the activating effects of retigabine were monitored. When the p.R331Q mutant was co-expressed with higher amounts of WT cDNA, the densities of retigabine-activated heteromeric currents increased, and those recorded at WT : p.R331Q ratios of 3:1 and 2:2 were comparable to homomeric WT currents (Fig. 8A and 8B).

Retigabine-activated currents were 37.63 ± 6.50, 34.26 ± 7.07, 33.23 ± 7.52, 11.54 ± 4.85, 10.66 ± 1.37, and -2.64 ± 1.05 pA/pF at WT : p.R331Q ratios of 4:0, 3:1, 2:2, 1:3, 0:4, and GFP, respectively (Fig. 8C). Overall, since the amount of p.R331Q cDNA increased compared to WT cDNA, the retigabine-activated heteromeric currents also decreased gradually. Importantly, I found that homomeric p.R331Q mutant channels (i.e., WT : p.R331Q ratio = 0:4), which is non-functional on its own, are activated by 30 μM retigabine. As opposed to the p.R331Q mutant, lower retigabine activation efficiency was observed in c811_816del mutant channels (Fig. 9). Homomeric c811_816del mutant channels (WT : c.811_816del ratio = 0:4) and 1:3 heteromeric channels were minimally activated by 30 μM retigabine (Fig. 9A and 9B). Heteromeric channels at a 3:1 ratio can be activated by retigabine. The obtained retigabine-activated currents were 37.63 ± 6.50, 30.91 ± 9.77, 12.28 ± 7.87, 3.98 ± 2.86, -2.33 ± 1.00, and -2.64 ± 1.05 pA/pF at WT : c.811_816del ratios of 4:0, 3:1, 2:2, 1:3, 0:4, and GFP, respectively (Fig. 9C).

Taken together, the data suggest that p.R331Q and c.811_816 del KCNQ4 channels are loss-of-function mutations that have dominant-negative effects when assembled with functional WT KCNQ4 channels. In addition, heteromeric mutant channels assembled with WT can be activated by the KCNQ4 activator retigabine, and the degree of retigabine activation is higher in p.R331Q heteromers than in c.811_816del heteromers.

Discussion

In this study, I identified two novel KCNQ4 mutations, p.R331Q and c.811_816del, in two Korean families. Since the first report in 1999 of an association between KCNQ4 and autosomal dominant non-syndromic HL [1], further studies have identified 21 KCNQ4 gene mutations [5]. The previously identified KNCQ4 mutants were located at diverse loci: 3 of 21 were in the N-terminal cytoplasmic tail, 1 was in the S3 transmembrane domain, 2 were in the S4 - S5 linker, 3 were in the S5 transmembrane domain, 10 were in the pore region, and 2 were in the S6 transmembrane domain. In addition, all mutations (excluding p.V230E) were associated with high frequency HL [5, 6]. As discussed above, no mutants have been found in the C-terminal tail showing an association with low- to mid-frequency HL. Therefore, it is important to note that our novel p.R331Q mutation is the first C-terminal tail variant showing a unique phenotype (i.e., an association with low- to mid-frequency HL). c811_816del is located in the pore region and shows an association with high-frequency HL, similar to previous mutants. However, all previous mutants located in the P-loop were shown to be 'missense' mutations, while c.811_816del is a 'deletion' mutant.

Regarding the phenotype-genotype correlation of KCNQ4, Wang et al. discussed how missense mutants typically lead to younger-onset HL involving all frequencies, while deletion mutants are associated with later-onset HL at high frequencies [4, 5]. However, this was not seen

in this study: the p.R331Q missense mutation showed an association with later-onset HL , and c.811_816del showed an association with earlier onset HL. This suggests that future studies on this topic should explore the phenotype rather than the type of mutation.

To explore the mechanisms underlying the mutations, I examined protein trafficking and synthesis and assessed membrane voltage using the patch-clamp method. Regarding p.R331Q, membrane expression did not differ WT; however, the membrane K^+ voltage was decreased. According to 3D protein modeling, the p.R331 residue in the C-terminus interacts with phosphatidyl inositol 4, 5-bisphosphate (PIP2). However, the guanine (R) to adenine (Q) transition inhibits this interaction and interferes with the homeostasis of membrane K^+ voltage, although protein synthesis remains normal. Regarding c.811_816del, membrane protein synthesis was decreased, such that membrane K^+ voltage consequently decreased, similar to what was seen in other P-region mutants [11-14]. The molecular mechanism underlying how KCNQ4 mutations result in a loss of function remains unclear. In 2006, Kharkovets et al. showed that the loss of function associated with KCNQ4 involved selective degeneration of OHCs and SGs in mouse models [15]. In 2013, Gao et al. explored the effects of seven loss-of-function DFNA2 mutations, all of which were situated in the P-loop, on the total protein level and cell surface expression of the KCNQ4 channel. They proposed two possible mechanisms: decreased cell surface expression (based on immunofluorescent microscopy and Western blot) and decreased

conductance of KCNQ4 (based on electrophysiological methods) [16].

In this study, when p.R331Q and c.811_816del were co-expressed with KCNQ4WT, the KCNQ4-mediated current was abolished, supporting their dominant-negative effects. Missense mutations are believed to have a dominant-negative effect by interrupting the normal KCNQ4 channel subunit [5]. Meanwhile, the deletion mutation is thought to exert a pathogenic influence through haploinsufficiency [17].

Most importantly, in this study, p.R331Q maintained a partial response to retigabine (KCNQ channel activator), which is suggestive of phenotypic rescue and represents a promising result for patients with autosomal non-syndromic HL. Regarding the phenotype rescue, one study showed that heat shock protein 90 (HSP90) promotes ubiquitin-dependent degradation of the KCNQ4 channel and is associated with the molecular chaperone that controls the KCNQ4 channel at the cellular level [18]. However, HSP90 is not assistive for both R331Q and 811_816del, since they are not degraded through the ubiquitin pathway (Fig. 4D and 4D′).

The PTA threshold at 8 kHz in patients with the p.R331Q mutation does not agree with the phenotype of HL. KCNQ4 is believed to be associated with age-related HL, since it progressively influences only the high frequencies, while the low frequencies remain normal until an old age [19]. Van Eyken et al. explored the relationship between KCNQ4 and age-related HL in Caucasian populations, and showed that all SNPs were located in the same 13 kb area within the

KCNQ4 gene, suggesting that the pathogenic mutants responsible for age-related HL may also be in this region [20].

This study had some limitations. First, the effects of each mutant on the assembly of KCNQ4 proteins were not evaluated. Thus, further studies using immunoprecipitation techniques are required. Second, the molecular mechanism underlying the mutations remains unclear, despite the functional implications of KCNQ4 mutations. Third, the molecular mechanism underlying the association between p.R331Q and low- to mid-frequency HL has not been determined.

In conclusion, I report a pathogenic variant in the KCNQ4 gene in the intracytoplasmic C-terminal tail for the first time. Furthermore, I extended the audiologic phenotypic spectrum of KCNQ4 mutations from high frequency sensorineural HL to include low- to mid-frequency sensorineural HL.

References

1. Kubisch C, Schroeder BC, Friedrich T, Lutjohann B, El-Amraoui A, Marlin S, et al. KCNQ4, a novel potassium channel expressed in sensory outer hair cells, is mutated in dominant deafness. Cell. 1999;96(3):437-46.

2. Coucke P, Van Camp G, Djoyodiharjo B, Smith SD, Frants RR, Padberg GW, et al. Linkage of autosomal dominant hearing loss to the short arm of chromosome 1 in two families. The New England journal of medicine. 1994;331(7):425-31.

3. Friedman TB, Griffith AJ. Human nonsyndromic sensorineural deafness. Annual review of genomics and human genetics. 2003;4:341-402. E

4. Nie L. KCNQ4 mutations associated with nonsyndromic progressive sensorineural hearing loss. Current opinion in otolaryngology & head and neck surgery. 2008;16(5):441-4.

5. Wang H, Zhao Y, Yi Y, Gao Y, Liu Q, Wang D, et al. Targeted high-throughput sequencing identifies pathogenic mutations in KCNQ4 in two large Chinese families with autosomal dominant hearing loss. PloS one. 2014;9(8):e103133.

6. Naito T, Nishio SY, Iwasa Y, Yano T, Kumakawa K, Abe S, et al. Comprehensive genetic screening of KCNQ4 in a large autosomal dominant nonsyndromic hearing loss cohort: genotype-phenotype correlations and a founder mutation. PloS one. 2013;8(5):e63231.

7. Beisel KW, Rocha-Sanchez SM, Morris KA, Nie L, Feng F, Kachar B, et al. Differential expression of KCNQ4 in inner hair cells and sensory neurons is the basis of progressive high-frequency hearing loss. The Journal of neuroscience 2005;25(40):9285-93.
8. King KA, Choi BY, Zalewski C, Madeo AC, Manichaikul A, Pryor SP, et al. SLC26A4 genotype, but not cochlear radiologic structure, is correlated with hearing loss in ears with an enlarged vestibular aqueduct. The Laryngoscope. 2010;120(2):384-9.
9. Choi BY, Park G, Gim J, Kim AR, Kim BJ, Kim HS, et al. Diagnostic application of targeted resequencing for familial nonsyndromic hearing loss. PloS one. 2013;8(8):e68692.
10. Choi BY, Stewart AK, Madeo AC, Pryor SP, Lenhard S, Kittles R, et al. Hypo-functional SLC26A4 variants associated with nonsyndromic hearing loss and enlargement of the vestibular aqueduct: genotype-phenotype correlation or coincidental polymorphisms? Human mutation. 2009;30(4):599-608.
11. Topsakal V, Pennings RJ, te Brinke H, Hamel B, Huygen PL, Kremer H, et al. Phenotype determination guides swift genotyping of a DFNA2/KCNQ4 family with a hot spot mutation (W276S). Otology & neurotology 2005;26(1):52-8.
12. Arnett J, Emery SB, Kim TB, Boerst AK, Lee K, Leal SM, et al. Autosomal dominant progressive sensorineural hearing loss due to a novel mutation in the KCNQ4 gene. Archives of otolaryngology-head & neck surgery. 2011;137(1):54-9.
13. Mencia A, Gonzalez-Nieto D, Modamio-Hoybjor S, Etxeberria

A, Aranguez G, Salvador N, et al. A novel KCNQ4 pore-region mutation (p.G296S) causes deafness by impairing cell-surface channel expression. Human genetics. 2008;123(1):41-53.

14. Van Camp G, Coucke PJ, Akita J, Fransen E, Abe S, De Leenheer EM, et al. A mutational hot spot in the KCNQ4 gene responsible for autosomal dominant hearing impairment. Human mutation. 2002;20(1):15-9.

15. Kharkovets T, Dedek K, Maier H, Schweizer M, Khimich D, et al. Mice with altered KCNQ4 K+ channels implicate sensory outer hair cells in human progressive deafness. European Molecular Biology Organization. 2006; 25: 642 - 52.

16. Gao YH, Yechikov S, Vazquez AE, Chen DY, Nie LP. Impaired surface expression and conductance of the KCNQ4 channel lead to sensorineural hearing loss. Journal of Cellular and Molecular Medicine. 2013;17:889 - 900.

17. Zhao YL, Zhao FF, Zong L, Zhang P, Guan LP, et al. Exome sequencing and linkage analysis identified tenascin-C (TNC) as a novel causative gene in nonsyndromic hearing loss. PLoS One. 2013; 8:e69549

18. Gao Y, Yechikov S, Vazquez AE, et al. Distinct roles of molecular chaperones HSP90alpha and HSP90beta in the biogenesis of KCNQ4 channels. PLoS ONE. 2013;8:e57282.

19. Coucke PJ, Van Hauwe P, Kelley PM, Kunst H, Schatteman I, et al. Mutations in the KCNQ4 gene are responsible for autosomal dominant deafness in four DFNA2 families. Human Molecular

Genetics. 1999;8: 1321-28.

20. Van Eyken E, Van Laer L, Fransen E, Topsakal V, Lemkens N, et al. KCNQ4: a gene for age-related hearing impairment? Human Mutation. 2006;1007 - 16.

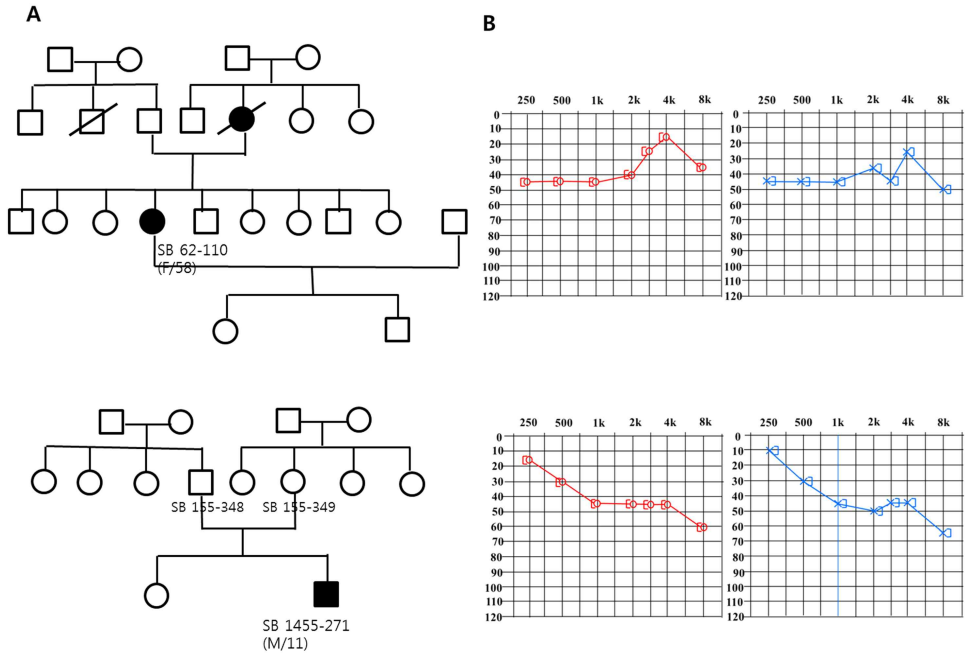

Fig. 1. Clinical information for each KCNQ4 mutant showing an association with autosomal dominant non-hereditary sensorineural hearing loss. (A) Pedigree of each KCNQ4 family. (B) Pure tone audiometry profile of each individual in the family.

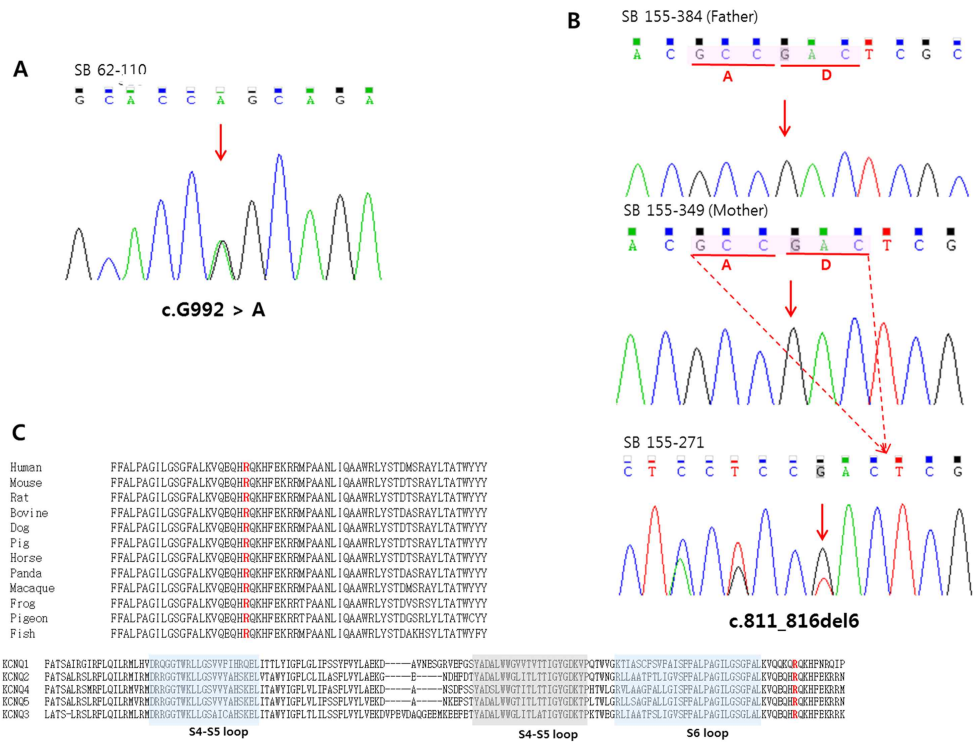

Fig. 2. Sanger sequencing traces for c.G992 〉 A (A) and c.811__816del (B), and conservation of the p.R331 residue among orthologs and paralogs (C).

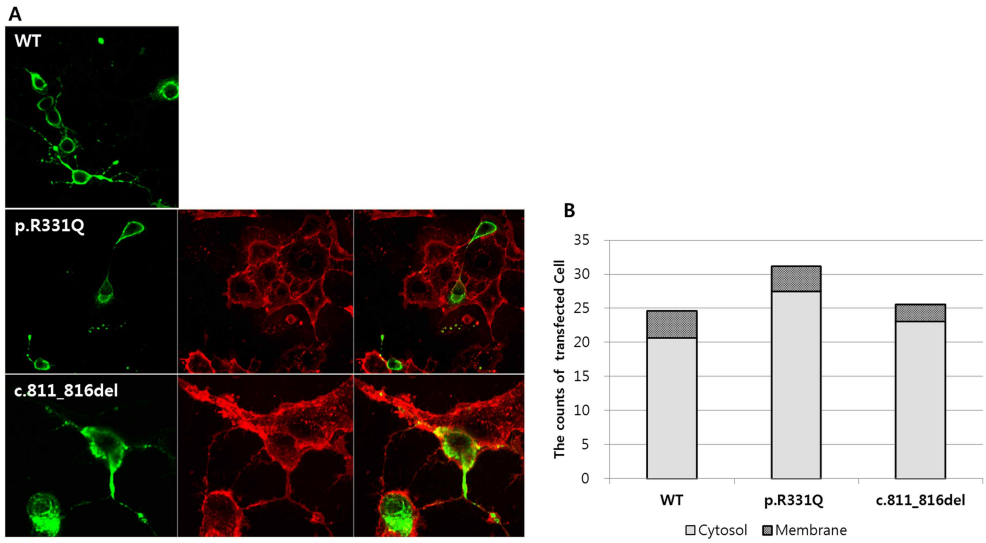

Fig. 3. Intracellular chemistry for wild-type *KCNQ4* (*KCNQ4*WT), the p.R331Q and c.811__816del mutations. *KCNQ4*WT and two mutants of *KCNQ4* showed no significant difference in the subcellular localization.

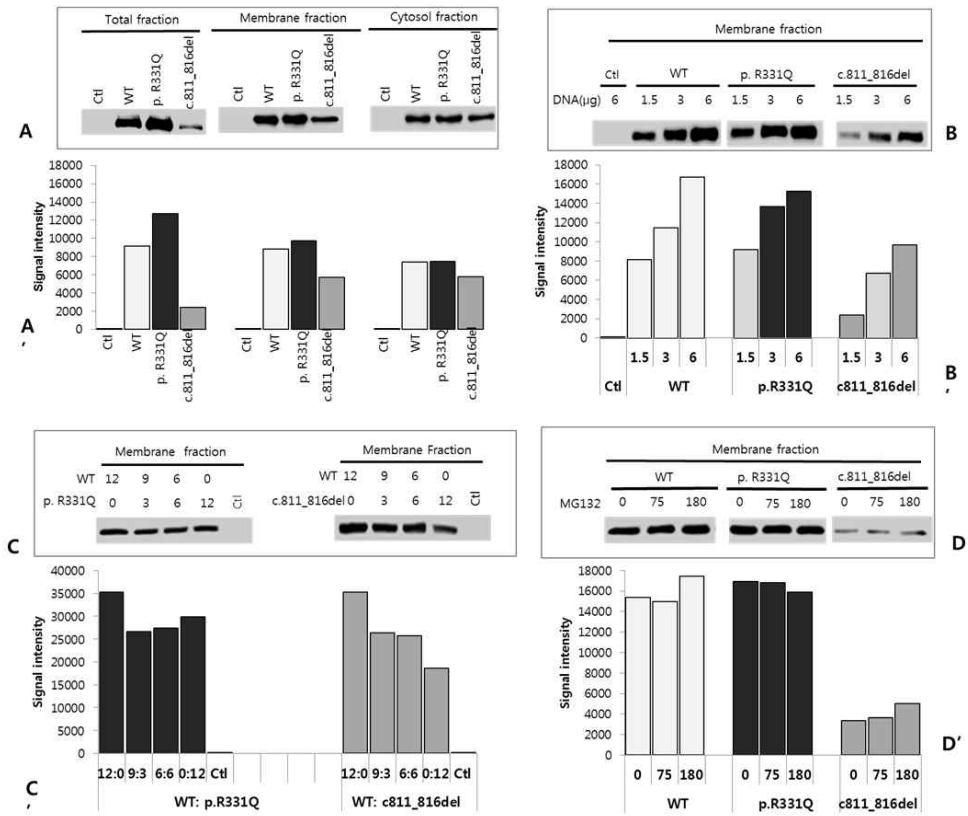

Fig. 4. Qualitative and quantitative expression analysis of total, membrane fraction, and cytosol KCNQ4 protein levels for KCNQ4WT, p.R331Q and c.811__816del mutations. (A) p.R331Q showed equal expression with the WT in the total and membrane fraction. However, that of c.811__816del was low. (B) As the DNA in WT, p.R331Q, and c.811__816del increased, did the synthesis of each protein. (C) For the cotransfection of WT and p.R331Q, it showed similar protein expression regardless of the mix ratio. For the cotransfection of WT and c.811__816del, the protein expression dropped, as the proportion of c.811_816del rose. (D) The protein expression levels were similar regardless of the amount of MG132 in all WT, p.R331Q and c.811_816del.

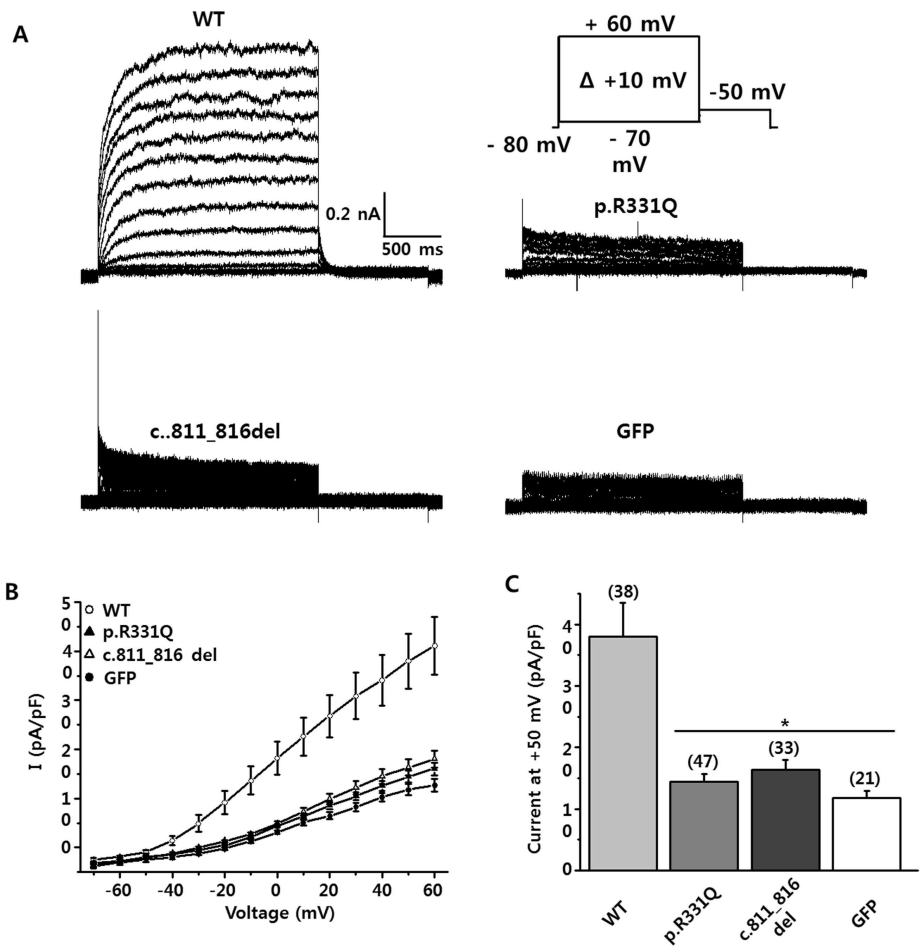

Fig. 5. Outward K+ currents recorded from HEK293 cells transiently expressed with human KCNQ4 channels. (A) Representative whole-cell current traces of green fluorescent protein (GFP), KCNQ4WT, KCNQ4p.R331Q, and KCNQ4c.811__816del. The applied voltage protocol is illustrated in the upper left panel. (B) Current-voltage (I-V) relationships obtained in each group. (C) Current densities measured at +50 mV are shown as bar graphs. *: $p < 0.05$ vs. WT.

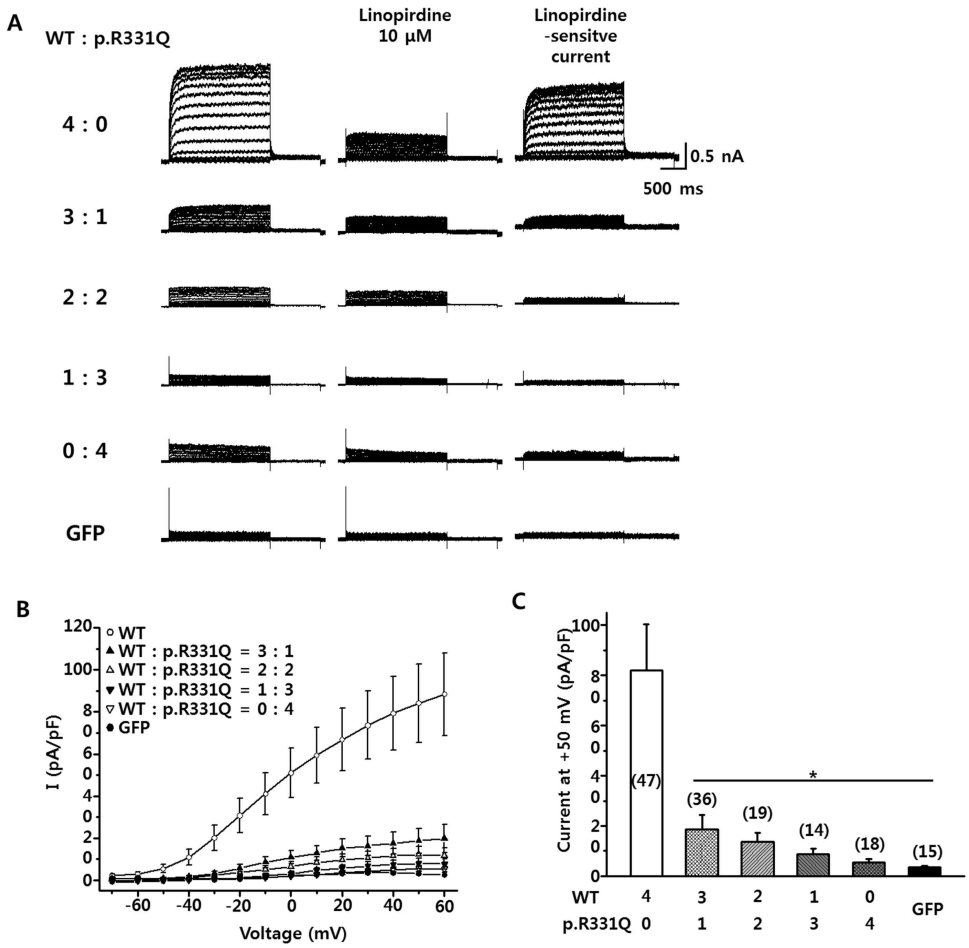

Fig. 6. Linopirdine-sensitive current measured in heteromeric p.R331Q KCNQ4 channels. (A) Representative whole-cell currents were demonstrated for KCNQ4WT and heteromeric KCNQ4p.R331Q, which was co-expressed with WT at the indicated ratios. Digital subtraction was done after treatment with linopirdine (10 μM), a KCNQ channel blocker. (B) I-V relationships obtained in each group. (C) Linopirdine-sensitive currents at +50 mV were obtained for each group and are shown as bar graphs. *: $p < 0.05$ vs. WT: p.R331Q = 4:0, #: $p < 0.05$ vs. GFP.

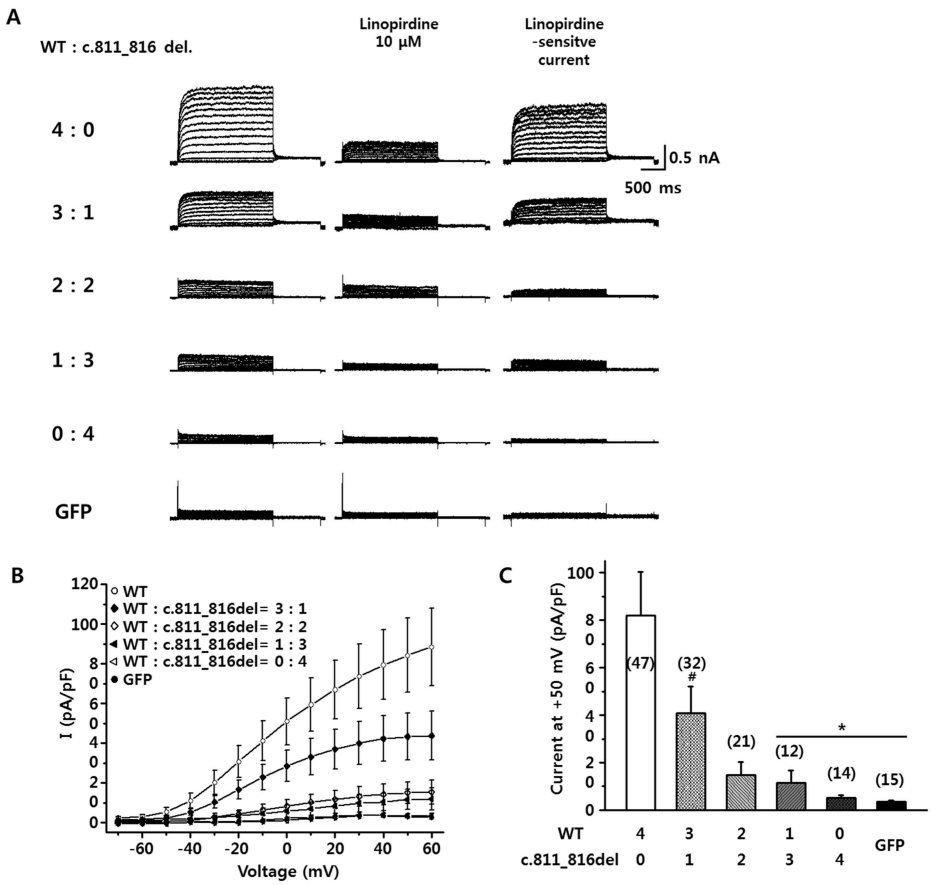

Fig. 7. Linopirdine-sensitive current measured in heteromeric c.811__816del KCNQ4 channels. (A) Representative whole-cell currents for KCNQ4WT and heteromeric KCNQ4c.811__816del, which was co-expressed with WT at the indicated ratios. Digital subtraction was done after treatment with linopirdine (10 μM), a KCNQ channel blocker. (B) I-V relationships obtained in each group. (C) The linopirdine-sensitive currents at +50 mV were obtained for each group and are shown as bar graphs. *: p< 0.05 vs. WT: c.811__816del = 4:0, #: p< 0.05 vs. GFP.

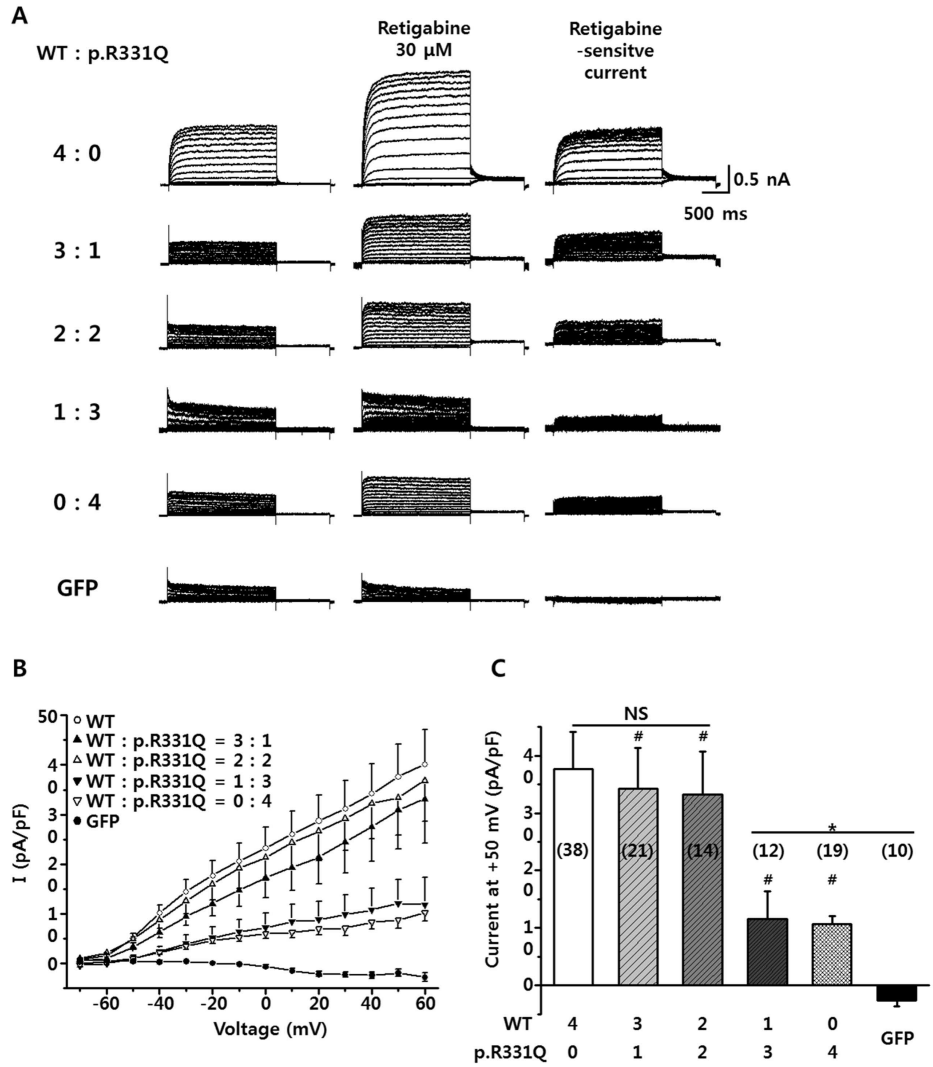

Fig. 8. Activation of heteromeric p.R331Q mutant channels by retigabine, a KCNQ channel activator. (A) Heteromeric KCNQ4p.R331Q channels were activated by retigabine (30 μM). After treatment with retigabine, digital subtracted retigabine-sensitive currents were seen. (B) I-V relationship of the retigabine-activated KCNQ4 current. (C) At +50 mV, the amplitudes of retigabine-activated KCNQ4 currents are shown as bar graphs. *: $p < 0.05$ vs. WT: p.R331Q = 4:0, #: $p < 0.05$ vs. GFP.

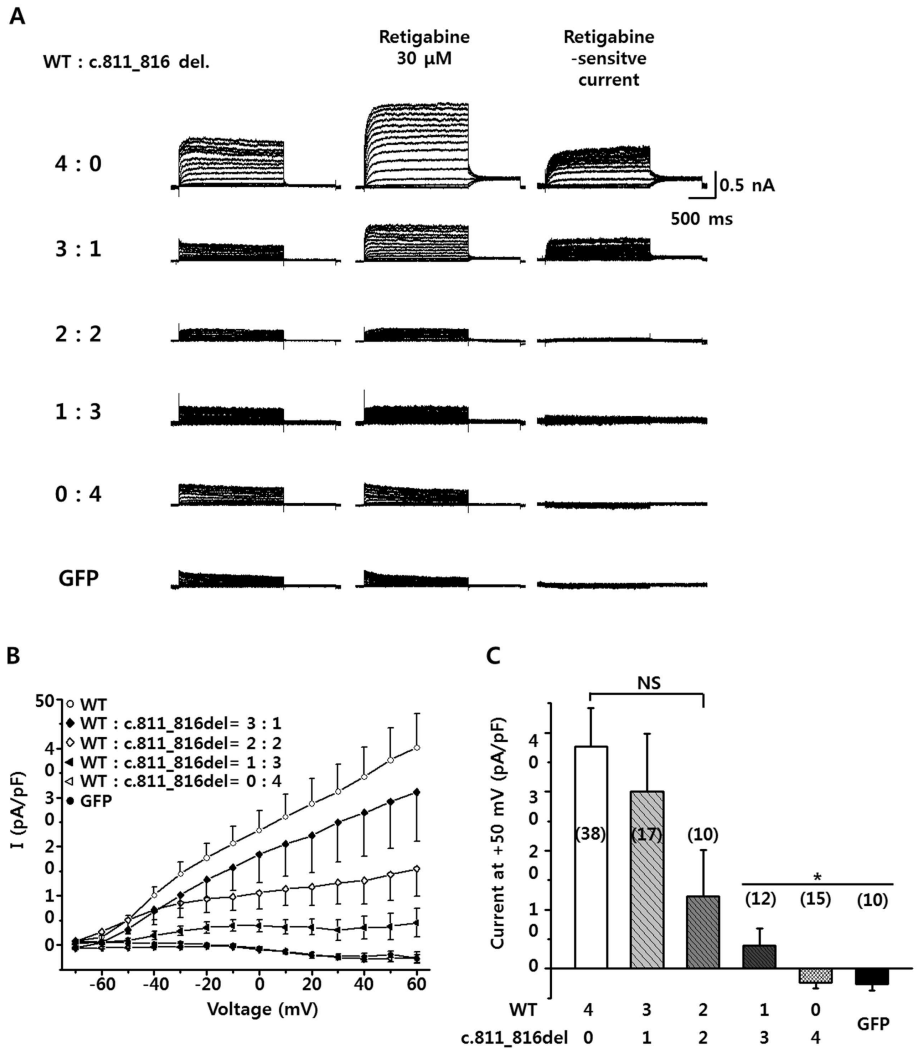

Fig. 9. Activation of heteromeric c.811__816del mutant channels by retigabine, a KCNQ channel activator. (A) Heteromeric KCNQ4c.811__816del channels were activated by retigabine (30 μM). After treatment with retigabine, digital subtracted retigabine-sensitive currents were seen. (B) I-V relationship of the retigabine-activated KCNQ4 current. (C) At +50 mV, the amplitudes of retigabine-activated KCNQ4 current are shown as bar graphs. *: p< 0.05 vs. WT: c.811__816del =4:0, #*: p< 0.05 vs. GFP.

국문 초록

KCNQ4 돌연변이는 비증후군성 상염색체 우성 난청을 유발하는 원인 유전자로, 일반적으로 진행성 고주파수 난청을 일으킨다. 본 연구에서 새로운 *KCNQ4* 돌연변이 두 종류 (p.R331Q와 p.811_816del)를 발견하였다. p.R331Q은 세포막 KCNQ4 단백질의 C 말단부에 위치하면서 저주파수대 난청을 보인 반면, p.811_816del은 P 고리에 위치하면서 고주파수대 난청을 보였다. 두 변이는 세포막 단백질 이동 과정에 야생형과 차이가 없었으나, 웨스턴 블롯 검사에서 c.811_816del은 야생형과 p.R331Q에 비해 단백질 합성이 뚜렷하게 감소되었다. 전기생리실험에서 두 개의 변이 모두 야생형에 비하여 세포막의 칼륨 전류가 저하되어 있어서 두 변이 모두 병적 변이일 가능성이 높았다. 두 변이를 각각 여러 비율로 야생형과 섞었을 때, 두 변이 모두 dominant negative effect를 보였다. 또한, 두 변이를 각각 여러 비율로 야생형과 섞은 후, *KCNQ4* activator (retigabine)를 넣었을 경우, p.R331Q heteromer의 세포막 전위가 c.811_816del heteromer 보다 뚜렷하게 많이 회복 되었다. 본 연구는 처음으로 발견된 C- 말단부에 위치하는 KCNQ4 돌연변이를 보고하였다. 또한, KCNQ4의 돌연변이가 저주파수 부터 중간 주파수 난청의 표현형을 보이는 경우 보고함으로써, KCNQ4 돌연변이 표현형의 범위를 확대하였다.

주요어: 난청, *KCNQ4*, 세포막 칼륨 채널, 세포막 전위, 돌연변이, Dominant negative effect

학 번: 2014-30928